Cancer Gene Therapy (2009) 16, 393–404
 0929-1903/09 $32.00
www.nature.com/cgt

ORIGINAL ARTICLE

Potentiation of methoxymorpholinyl doxorubicin antitumor activity by *P*450 3A4 gene transfer

H Lu[1], C-S Chen[1] and DJ Waxman

Division of Cell and Molecular Biology, Department of Biology, Boston University, Boston, MA, USA

Preclinical and clinical studies of *CYP* gene-directed enzyme prodrug therapy have been focused on anticancer prodrugs activated by CYP2B enzymes, which have low endogenous expression in human liver; however, the gene therapeutic potential of CYP3A enzymes, which are highly expressed in human liver, remains unknown. This study investigated methoxymorpholinyl doxorubicin (MMDX; nemorubicin), a novel CYP3A-activated anticancer prodrug. Retroviral transfer of *CYP3A4* increased 9L gliosarcoma cell chemosensitivity to MMDX 120-fold ($IC_{50} = 0.2$ nM in 9L/3A4 cells). In CHO cells, overexpression of *P*450 reductase in combination with CYP3A4 enhanced chemosensitivity to MMDX, and to ifosfamide, another CYP3A4 prodrug, 11- to 23-fold compared with CYP3A4 expression alone. CYP3A4 expression and MMDX chemosensitivity were increased in human lung (A549) and brain (U251) tumor cells infected with replication-defective adenovirus encoding *CYP3A4*. Coinfection with Onyx-017, a replication-conditional adenovirus that coamplifies and coreplicates the Adeno-3A4 virus, led to large increases in CYP3A4 RNA but only modest increases in CYP3A4 protein and activity. MMDX induced remarkable growth delay of 9L/3A4 tumors, but not the *P450*-deficient parental 9L tumors, in immunodeficient mice administered low-dose MMDX either intravenous or by direct intratumoral (i.t.) injection (60 μg kg^{-1}, every 7 days × 3). Notably, the i.t. route was substantially less toxic to the mouse host. No antitumor activity was observed with intraperitoneal MMDX treatment, suggesting a substantial hepatic first pass effect, with activated MMDX metabolites formed in the liver having poor access to the tumor site. These studies demonstrate that human CYP3A4 has strong potential for MMDX prodrug-activation therapy and suggest that endogenous tumor cell expression of CYP3A4, and not hepatic CYP3A4 activity, is a key determinant of responsiveness to MMDX therapy in cancer patients *in vivo*.
Cancer Gene Therapy (2009) **16,** 393–404; doi:10.1038/cgt.2008.93; published online 14 November 2008

Keywords: methoxymorpholinyl doxorubicin; nemorubicin; CYP3A4; gene-directed enzyme prodrug therapy; prodrug-activation gene therapy

Introduction

Genes encoding prodrug-activation enzymes, when expressed in tumor cells, confer the ability to metabolize an inactive anticancer prodrug into a potent cytotoxin. The cytotoxic metabolite not only kills the enzyme-expressing cells *in situ*, but may also diffuse into neighboring cells, thereby inducing a bystander cytotoxic response.[1,2] This strategy serves as the basis for prodrug-activation gene therapy using liver cytochrome *P*450 (CYP)-activated anticancer prodrugs, such as cyclophosphamide, which have the potential to achieve selective delivery of activated prodrugs to tumor tissue while minimizing systemic metabolism, thereby reducing host toxicity.[3] Enzyme–prodrug combinations that have been evaluated in preclinical studies include CYP2B enzymes together with *P*450 reductase[4] in combination with cyclophosphamide,[5–8] herpes simplex virus thymidine kinase with ganciclovir as the prodrug, cytosine deaminase with 5-fluorocytosine, carboxylesterase with irinotecan, thymidine phosphorylase with 5-deoxyfluorouridine, purine nucleoside phosphorylase with 6-methylpurine derivatives and nitroreductase with CB1954.[9–11] Thymidine kinase/ganciclovir and cytosine deaminase/5-fluorocytosine have been tested in clinical trials[12–14] as has CYP2B6 in combination with oral cyclophosphamide in patients with advanced breast cancer or malignant melanoma, where clinical indications of efficacy were reported.[15] Other *P*450 prodrugs investigated in preclinical gene therapy studies include ifosfamide (IFA),[16,17] an isomer of cyclophosphamide, and the bioreductive drugs tirapazamine[18] and AQ4N.[19]

Methoxymorpholinyl doxorubicin (MMDX; nemorubicin) is a derivative of doxorubicin that displays enhanced cytotoxicity toward human tumor cells and hematopoietic progenitors when incubated with liver microsomes, which contain high *P*450 metabolic activity.[20,21] The potentiation of MMDX activity is due to

Correspondence: Dr DJ Waxman, Division of Cell and Molecular Biology, Department of Biology, Boston University, 5 Cummington St, Boston, MA 02215, USA.
E-mail: djw@bu.edu
[1]These authors contributed equally to this work.
Received 17 June 2008; revised 3 August 2008; accepted 12 September 2008; published online 14 November 2008

metabolic activation by liver-expressed CYP3A enzymes.[22–24] The *P*450-generated active metabolite of MMDX was recently identified and shown to have much higher potency toward cultured cells, and remarkable effectiveness toward tumor xenografts in nude mice, compared with MMDX.[25] Activated MMDX retains activity against tumor cells with different mechanisms of resistance to classical anticancer agents, including MMDX itself.[26,27] Troleandomycin, a CYP3A enzyme-selective inhibitor, blocks hepatic MMDX activation, thereby decreasing antitumor activity and bone marrow toxicity, demonstrating that activated MMDX contributes to both antitumor activity and host toxicity *in vivo*.[28] Consequently, strategies to reduce systemic MMDX exposure need to be developed to optimize the therapeutic index of this novel anthracycline prodrug.

In an earlier study, CYP3A4 was shown to be the most active catalyst of MMDX activation in a panel of rat and human CYP3A enzymes.[27] Presently, we evaluate the therapeutic impact of introducing *CYP3A4* into tumor cells in combination with MMDX treatment *in vitro* and *in vivo*. In addition, we employ a replication-defective adenovirus to facilitate *CYP3A4* gene transfer to human tumor cells. The potential utility of a replication-conditional adenovirus to enhance *CYP3A4* gene delivery was also investigated. Our findings demonstrate the striking therapeutic potential of CYP3A4 in combination with MMDX treatment and, furthermore, suggest that endogenous tumor cell expression of CYP3A4 in individual patients may serve as an important determinant of responsiveness to MMDX *in vivo*.

Materials and methods

Supplementary materials and methods

Materials and methods used for western blotting, *P*450 reductase assay, quantitative real-time PCR analysis, CYP3A4 adenovirus preparation and adenovirus-mediated RNA transcription, protein expression and enzyme activity are available on-line as Supplementary Information.

Cell lines

CHO/HR, CHO/3A4 and CHO/3A4/HR cells[29] were obtained from Dr Thomas Friedberg (Biomedical Research Centre, University of Dundee, UK) and were grown in α-MEM culture medium containing dialyzed 10% fetal bovine serum (FBS) (CHO/3A4 and CHO/3A4/HR cells) or in Dulbecco's modified Eagle's medium (DMEM) containing 10% FBS, 10 mM hypoxanthine and 1.6 mM thymidine (Invitrogen, Carlsbad, CA). 9L and 9L/3A4 cells (see below) were cultured in DMEM + 10% FBS. Human tumor cell lines U251 (brain tumor) and A549 (lung cancer) were obtained from Dr Dominic Scudiero (NCI, Bethesda, MD).

Generation of 9L/3A4 cells by retroviral infection

CYP3A4 cDNA, obtained by reverse transcriptase PCR of human liver RNA and cloned in the *Xho*I/*Xba*I sites of pDHFR to yield pDHFR/3A4, was kindly provided by Dr Thomas Friedberg. The nucleotide sequence flanking the AUG initiator codon of CYP3A4 was modified to conform to the conserved Kozak sequence XX(A/G)XXAUGG, required for the efficient initiation of eukaryotic protein synthesis.[30] A retroviral plasmid of the pBabe series, which encodes a puromycin resistance gene transcribed from the SV40 early promoter, was obtained from Dr B Spiegelman (Dana-Farber Cancer Institute, Boston, MA). CYP3A4 excised from pDHFR/3A4 with *Xho*I and *Xba*I was blunt ended and subcloned into the blunt-ended *Sna*BI site of pBabe-puro to yield pBabe-puro-3A4, where *CYP3A4* transcription is regulated by the retroviral long-terminal repeat promoter. To generate infectious retroviral particles, the ecotropic packaging cell line Bosc 23 was cultured at 2.5×10^6 cells per 60-mm dish in 4 ml of DMEM (Invitrogen) containing 10% FBS, 100 U ml^{-1} penicillin and 100 μg ml^{-1} streptomycin (Invitrogen). pBabe-puro-3A4 DNA (5 μg) and pKAT DNA (2 μg)[31] were cotransfected into Bosc 23 cells using Fugene 6 transfection reagent (Roche Diagnostics, Indianapolis, IN) according to the manufacturer's instructions. Cells were cotransfected with pBabe-puro + pKAT as a *P*450-deficient control. Twenty-four hours later, the culture medium was replaced with 4 ml of fresh DMEM containing 10% FBS. After a second 24-h period, the culture medium, containing infectious retroviral particles, was gently removed with a sterile pipette and added to 9L gliosarcoma cells (5×10^5 cells in a 100-mm dish) in the presence of 4 μg ml^{-1} of polybrene (Sigma-Aldrich, St Louis, MO). Three hours later, the medium was supplemented with 7 ml of fresh DMEM + 10% FBS. The infected 9L cells were trypsinized 48 h later, split into four 100-mm dishes and treated with 2 μg ml^{-1} puromycin for 3 days. Approximately 80% of the infected 9L cells acquired resistance to puromycin, indicating a high efficiency of retroviral gene delivery. Pools of puromycin-resistant cells were grown in puromycin-free medium and assayed for CYP3A4 protein (western blot analysis) and MMDX sensitivity. To select clonal 9L/3A4 cells, a puromycin-resistant 9L/3A4 cell pool was trypsinized and diluted to a nominal density of one, two and four cells per 200 μl of DMEM containing 10% FBS and plated in 96-well plates. Wells containing single colonies were identified ~2 weeks later using a light microscope, trypsinized and divided into duplicate wells of a 24-well plate. One well derived from each colony was kept untreated, and the second well was treated with 5 nM MMDX for 4 days. Six of the 30 colonies examined were killed by MMDX with a high efficiency (100% cell killing after 4 days). Wells containing untreated cells derived from the corresponding colonies were trypsinized and replated into six-well plates for propagation and further characterization. All experiments using 9L/3A4 cells were carried out using 9L/3A4 clone 5 (see Figure 1a, below). The term '9L cells' refers to a pool of puromycin-resistant 9L cells infected with pBabe-puro, which was used as a *P*450-deficient control.

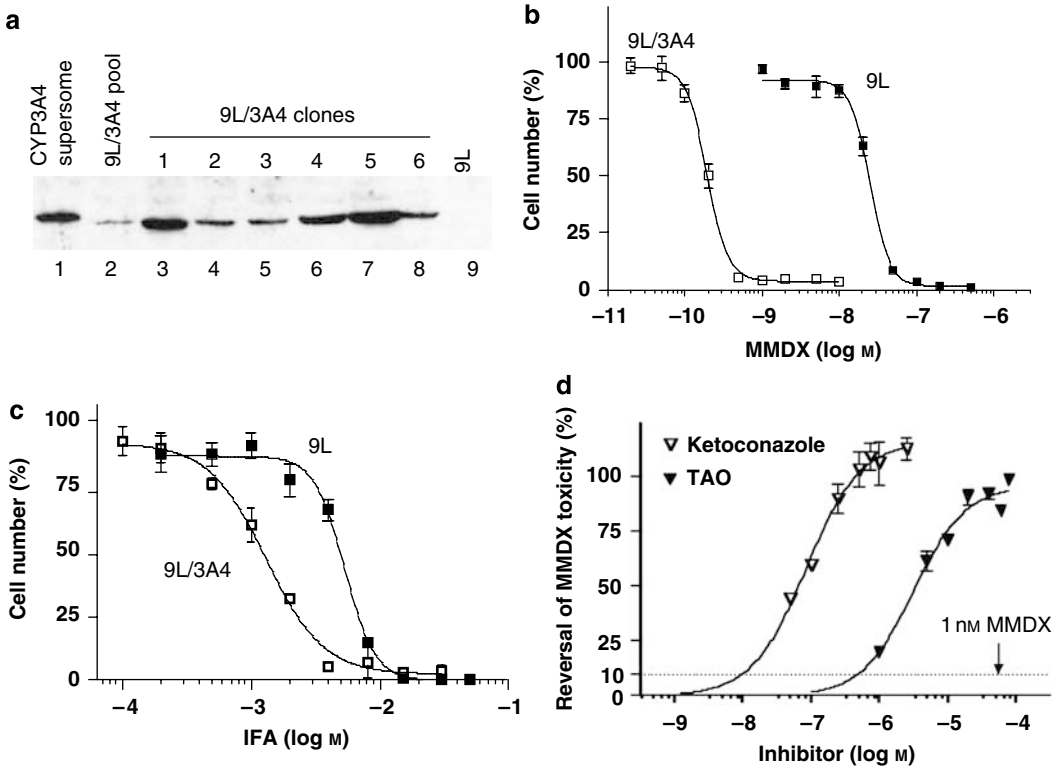

Figure 1 Chemosensitivity of 9L/3A4 cells to MMDX and IFA. (**a**) CYP3A4 western blot of total cellular protein (60 μg per well; 10% SDS-polyacrylamide gel). Lane 1, baculovirus-expressed CYPA3A4 (supersomes) protein standard (0.5 pmol *P*450); lane 2, original puromycin-selected 9L/3A4 retroviral pool; lanes 3–8, individual 9L/3A4 clones, numbered 1–6 above the gel and selected based on enhanced MMDX sensitivity; lane 9, wild-type 9L cells. Quantitation of CYP3A4 protein levels using ImageQuant software (Molecular Dynamics, Sunnyvale, CA) based on lymphoblast-expressed CYP3A4 standard yields a CYP3A4 protein content of 15.3 pmol *P*450 per mg cellular protein in clone 5. (**b** and **c**) Chemosensitivity of 9L/3A4 (clone 5) and 9L cells to MMDX (**b**) and IFA (**c**) determined in a 4-day growth inhibition assay. Relative cell number, expressed as a percentage of drug-free controls, was determined by crystal violet staining. IC_{50} values determined in this and similar experiments are listed in Table 1. (**d**) Cytotoxicity of 1 nM MMDX toward 9L/3A4 cells (clone 5) in a 4-day growth inhibition assay was blocked in a concentration-dependent manner by the CYP3A inhibitors troleandomycin (TAO) and ketoconazole with EC_{50} values of 5 μM and 50 nM, respectively. Horizontal dashed line represents 90% cell killing of 9L/3A4 cells at 1 nM MMDX. Data shown are mean values ± s.d. ($n = 3$). IFA, ifosfamide; MMDX, methoxymorpholinyl doxorubicin.

Cell growth inhibition assay

9L and CHO cells were plated in triplicate wells of a 96-well plate at 3000 cells per well 24 h before drug treatment. Cells were treated with various concentrations of MMDX or IFA for 4 days. Cells were then stained with crystal violet (A_{595}) and relative cell survival was calculated.[27] IC_{50} values were determined from a semi-logarithmic graph of the data points using Prism 4 (Graphpad Software Inc., San Diego, CA).

Quantitation of 4-OH-IFA production and active MMDX formation by tumor cells expressing CYP3A4

9L/3A4 cells were plated in 12-well culture plates at 1.5×10^5 cells per well in 1.5 ml culture medium. Twenty-four hours later, IFA at various concentrations was added to the cells together with 5 mM semicarbazide to trap and stabilize the 4-OH-IFA metabolite. After 4 h of treatment, an aliquot of culture medium (0.5 ml) was removed from each well and stored at −80 °C until ready for 4-OH-IFA analysis. Cells remaining on the plate were washed with phosphate-buffered saline and stained with crystal violet. A C_{18} high-performance liquid chromatography assay was used to quantify 4-OH-IFA by fluorescence after derivatization of its by-product acrolein to 7-hydroxyquinoline.[32] Standard curves for 4-OH-CPA were generated using 4-OOH-CPA dissolved in cell culture medium (0–40 μM).[32] Cellular IFA 4-hydroxylase activity was calculated from integrated peak areas determined by Millennium 32 software.

CYP3A4-activated MMDX metabolite released into the culture medium was assayed as follows. 9L and CHO cells expressing CYP3A4, and CYP3A4-deficient control cells, were plated in 12-well plates at 1.5×10^5 cells per well. Twenty-four hours later, MMDX at various concentrations was added to the cells in 1.5 ml culture medium for 2 h, at which time 0.5 ml of the culture supernatant was removed from the 9L and 9L/3A4 cell cultures and mixed with 0.5 ml of fresh α-MEM + 10% dialyzed FBS. In parallel, 0.5 ml of culture supernatant was removed from the MMDX-treated CHO cell lines and mixed with 0.5 ml of fresh DMEM + 10% FBS. A 0.2 ml aliquot of each sample was added to triplicate wells of 9L cells, seeded 24 h earlier at 3000 cells per well in 96-well plates ('9L indicator cells'). The 9L indicator cells

were cultured for 4 days in the 0.2 ml medium containing MMDX metabolites and then stained with crystal violet to determine relative cell numbers as an index of the level of active MMDX metabolite formed by each cell line during the initial 2 h MMDX incubation period.

Adenoviral infection of human tumor cell lines and MMDX cytotoxicity assays

A549 and U251 cells were plated in 24-well plates at 14 000 cells per well and infected 24 h later with Adeno-3A4 (multiplicity of infection (MOI) 0–400) either alone or in combination with Onyx-017 (MOIs 0, 0.7 and 2). The cells were incubated with the viruses for 4 h in 0.2 ml culture medium per well, after which 0.8 ml of fresh medium was added to each well. The virus was removed after 24 h, and 1 ml of fresh medium containing MMDX (0–8 nM) was added to the cells. After 2 days of MMDX treatment, the medium was replaced with 1 ml of fresh MMDX-containing medium for an additional 4 days. Surviving cells were stained with crystal violet.

Tumor growth delay assay

9L and 9L/3A4 cells were grown as solid tumors in male ICR/Fox Chase SCID mice (Taconic Inc., Germantown, NY) using procedures approved by the Boston University Institutional Animal Care and Use Committee. Cells cultured in DMEM medium to 75% confluence were trypsinized and washed in phosphate-buffered saline and then adjusted to 2×10^7 cells per ml of FBS-free DMEM. Four-week-old SCID mice (18–20 g) were implanted with either 9L or 9L/3A4 tumor cells by injection of 4×10^6 cells per 0.2 ml of cell suspension, subcutaneously, on each hind flank. Tumor sizes (length and width) were measured twice a week using vernier calipers beginning from 7 days after tumor implantation. When the average tumor size reached 300–400 mm^3, MMDX dissolved in phosphate-buffered saline was administered by tail vein injection (intravenous, i.v.) or by direct intratumoral (i.t.) injection (three injections spaced 7 days apart, each at 60 μg MMDX per kg body weight, except as noted). I.t. injections were performed using a syringe pump (model 70–2212, Dual Syringe Pump with Serial Communication; Harvard Apparatus Inc., Holliston, MA) set at 1 μl s^{-1} with a 30-gauge needle. Each i.t. treatment dose was divided into three injections per tumor, with the injected volume set at 50 μl per tumor per 25 g mouse. Thus, for a 30 g mouse, a total of 120 μl of 15 μg ml^{-1} MMDX solution was administered: 20 μl per site × three sites per tumor × two tumors per mouse. For a 25 g mouse, a total of 100 μl of 15 μg ml^{-1} MMDX solution was administered: 50 μl per tumor, 16.7 μl per site × three sites per tumor × two tumors per mouse. Drug-free controls were injected i.t. with the same volume of phosphate-buffered saline. In some experiments, MMDX was administered by intraperitoneal (i.p.) injection at 40 or 60 μg per kg body weight. Tumor sizes and body weights were measured twice a week for the duration of the study. Tumor volumes were calculated using the formula: $V = \pi/6 (L \times W)^{3/2}$. Percent tumor regression was calculated as $100 \times (V_1 - V_2)/V_1$, where V_1 is the tumor volume on the day of drug treatment and V_2 is the volume on the day when the largest decrease in tumor size is seen following drug treatment. Tumor-doubling time was calculated as the time required for tumors to double in volume after drug treatment.

Results

Retroviral expression of human CYP3A4 chemosensitizes 9L gliosarcoma cells to MMDX and IFA

Retrovirus encoding CYP3A4 cDNA was used to infect 9L tumor cells, which were selected based on their acquired resistance to puromycin. CYP3A4 protein was detected in the resultant pool of puromycin-resistant cells, as shown by western blotting (Figure 1a). The selection of cells showing increased sensitivity to MMDX yielded clones with elevated levels of CYP3A4 protein. 9L/3A4 clone 5 had the highest CYP3A4 protein content,

Table 1 Cytotoxicity of MMDX and IFA and their activated metabolites toward 9L and CHO tumor cell lines

	IC_{50} (nM)		IC_{50} (μM)	
	MMDX	*MMDX+Dex microsomes*	*IFA*	*4-OOH-IFA*
9L	23.9	0.6	4900	8.9
9L/3A4	0.2 *(120x)*	ND	1230 *(4x)*	4.6
CHO/HR	58.8	2.2	4460	9.1
CHO/3A4	2.2, 4.4	ND	3460, 3550	4.7, 4.7
CHO/3A4/HR	0.29 *(11.3x)*	ND	151 *(23x)*	6.6

Abbreviations: IFA, ifosfamide; MMDX, methoxymorpholinyl doxorubicin; ND, not determined.

Shown are IC_{50} values determined with 9L and CHO cell lines that expressed CYP3A4 and/or human P450 reductase (HR). CHO/HR and 9L cells infected with the P450-deficient retroviral vector pBabe-puro were used as CYP3A4-negative controls. Assays were carried out with MMDX; with MMDX+dexamethasone-induced rat liver microsomes (2 μg microsomal protein per well) plus 0.3 mM NADPH, generating activated MMDX *in situ*[24]; with IFA; and with 4-OOH-IFA, which spontaneously decomposes to the active IFA metabolite, 4-OH-IFA. Each IC_{50} value was determined in a 4-day growth inhibition assay from dose–response curves that include triplicate samples at each of nine drug concentrations. Data shown are representative of two or more independent experiments similar to those shown in Figures 1b and c. Values shown for CHO/3A4 cells are for two independent clones with similar CYP3A4 protein content (clones CHO/3A4-4 and CHO/3A4-10). Values shown in parentheses are fold differences in IC_{50} values for 9L/3A4 cells vs 9L cells, and for CHO/3A4/HR cells vs CHO/3A4 cells.

15.3 pmol of CYP3A4 per mg total cellular protein, and was used in all subsequent experiments. The IC_{50} value of MMDX toward 9L/3A4 cells, 0.2 nM, was 120-fold lower than that of *P*450-deficient 9L cells ($IC_{50} = 23.9$ nM) (Figure 1b and Table 1). This potent cytotoxicity of activated MMDX contrasts with that of the CYP3A4 prodrug IFA, which required millimolar concentrations to kill 9L/3A4 cells (Figure 1c and Table 1). To verify the role of CYP3A4 metabolism in the activation of MMDX to cytotoxic metabolites, 9L/3A4 cells were treated with MMDX (1 nM) together with increasing concentrations of the CYP3A4 inhibitors ketoconazole and troleandomycin. MMDX cytotoxicity was fully blocked by ketoconazole (0.5 μM) and troleandomycin (20 μM) (Figure 1d).

P*450 reductase overexpression enhances cytotoxicity of MMDX and IFA*

*P*450 reductase is a rate-limiting component for microsomal *P*450 reactions,[33] including those catalyzed by CYP3A enzymes. We therefore investigated whether the cytotoxicity of MMDX could be further increased by the overexpression of *P*450 reductase. Efforts to augment the endogenous *P*450 reductase of 9L/3A4 cells by infection with retrovirus encoding rat *P*450 reductase were unsuccessful and resulted in a small decrease in CYP3A4 protein (data not shown). We therefore examined CHO cell lines engineered to express CYP3A4 alone (CHO/3A4 cells) or in combination with *P*450 reductase (CHO/3A4/HR cells).[29] These cells have CYP3A4 protein levels similar to each other and to 9L/3A4 cells (Figure 2a). *P*450 reductase activity was 31-fold higher in CHO/3A4/HR cells than in CHO/3A4 cells; it was also sixfold higher than in 9L/3A4 cells (Figure 2b). Correspondingly, CHO/3A4/HR cells showed a large increase in IFA metabolic activity, 28-fold compared with CHO/3A4 cells and 15-fold compared with 9L/3A4 cells (Figure 2c). CHO/3A4/HR cells also showed an increased MMDX activation, as determined by the formation of metabolites cytotoxic toward 9L indicator cells. Thus, at 4 nM MMDX, CHO/3A4/HR cells produced sufficient active metabolites to kill $>70\%$ of the 9L indicator cells, whereas $<10\%$ of indicator cell killing was observed with CHO/3A4 and 9L/3A4 cell lines under the same conditions (Figure 2d). Moreover, CHO/3A4/HR cells were $\sim$11.3-fold more sensitive to MMDX than CHO/3A4 cells (Table 1), where the low endogenous *P*450 reductase limits *P*450 metabolic activity. CHO/3A4/HR cells also exhibited 8- to 23-fold greater sensitivity to IFA, as compared with CHO/3A4 and 9L/3A4 cells (Table 1). All three cell lines exhibited similar intrinsic sensitivities to activated IFA ($<$2-fold difference in IC_{50} values; Table 1, last column) as determined using 4-OOH-IFA, a chemically activated form of IFA. Thus, the endogenous CHO tumor cell level of *P*450 reductase is rate limiting for CYP3A4-catalyzed activation of both MMDX and IFA.

Adeno-3A4 infection of human tumor cell lines

Adeno-3A4, an E1 and E3 region-deleted, replication-defective adenovirus encoding full-length CYP3A4 cDNA, was used to induce CYP3A4 expression in two human tumor cell lines, A549 lung and U251 brain cancer cells. U251 cells are more susceptible to adenovirus infection than A549 cells, as determined using adenovirus encoding bacterial β-galactosidase, visualized by staining the infected cells with the chromophoric substrate X-gal (data not shown). At an Adeno-3A4 MOI of 150, CYP3A4 RNA increased up to $\sim$6000-fold in both cell lines, as determined by quantitative real-time PCR (Supplementary Figure S1A). CYP3A4 RNA levels in the Adeno-3A4-infected cells (MOI 75) were similar to those found in 9L/3A4 cells. Adeno-3A4 also induced a dose-dependent increase in CYP3A4 protein (Supplementary Figures S1B and S2) and metabolic activity, assayed by the formation and release of 4-OH-IFA into the culture medium of cells incubated with IFA (Supplementary Figure S1C). Overall, 4-OH-IFA production per pmol of CYP3A4 protein was two- to fourfold higher in 9L/3A4 cells than in the Adeno-3A4-infected A549 and U251 cells.

Adeno-3A4 infection conferred dose-dependent increases in MMDX toxicity toward U251 cells ($IC_{50} = 1.4$ nM at 100 MOI Adeno-3A4; Figure 3a). MMDX was cytotoxic to the Adeno-3A4-infected A549 cells, but only at high viral doses ($IC_{50} = 4.7$ nM at 200 MOI; Figure 3b) (c.f., IC_{50} (MMDX) = 24 nM in A549 controls[27]). In an effort to chemosensitize the cells to MMDX at lower Adeno-3A4 MOIs, cells were coinfected with Onyx-017, an E1B-55kd-deleted oncolytic adenovirus that selectively replicates in p53-deficient tumor cells and can be used as a helper virus to coamplify and increase the expression and cellular transmission of replication-defective virus encoding CYPs 2B6 and 2B11.[6,34] Coinfection of A549 or U251 tumor cells with Adeno-3A4 + Onyx-017 resulted in up to a 50- to 60-fold increase in CYP3A4 RNA compared with infection with Adeno-3A4 alone (Supplementary Figure S3A) accompanied by large increases in adenoviral E3 RNA, derived from Onyx-017 (Supplementary Figure S3B). However, only modest increases in CYP3A4 protein were obtained, although increased expression of a higher molecular weight CYP3A4 immunoreactive protein was also observed in cells infected with both viruses (Supplementary Figure S2). Onyx-017 increased Adeno-3A4-dependent CYP3A4 metabolic activity (Supplementary Figure S3C) and CYP3A4-dependent MMDX cytotoxicity (Figure 3c), albeit to a much lesser extent than the increase in CYP3A4 RNA (Supplementary Figure S3A).

Impact of CYP3A4 on MMDX antitumor activity in vivo

9L/3A4 cells were used as an *ex vivo* gene transfer model to evaluate the impact of *CYP3A4* gene delivery on the chemosensitivity of 9L tumors to MMDX *in vivo* in the context of endogenous liver MMDX metabolism. Figure 4 shows the results of a tumor growth delay study comparing the antitumor activity of MMDX toward 9L tumors vs 9L/3A4 tumors. Mice were given a series of three weekly injections of MMDX (60 μg per kg body weight) by i.v. injection or by direct i.t. injection. 9L tumors did not show any sustained growth delay in response to MMDX treatment through either injection

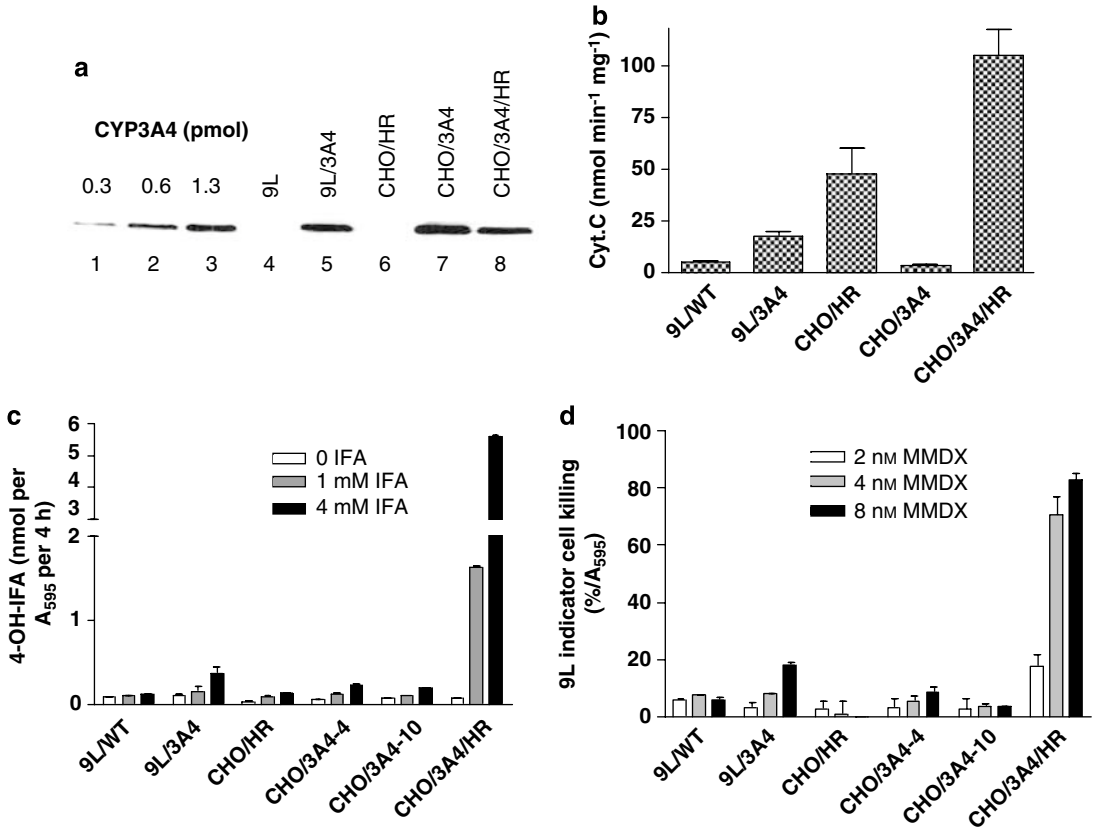

Figure 2 Metabolic activation of IFA and MMDX by CHO and 9L cells expressing CYP3A4 and/or *P*450 reductase (HR). (**a**) Western blot of CYP3A4 protein levels in CYP3A4 standards (lanes 1–3) and in each of the indicated cell lines (lanes 4–8), and (**b**) *P*450 reductase activity (cytochrome *c* reduction) were both determined in total cell lysates prepared from cells plated overnight in six-well tissue culture plates at 300 000 cells per well and collected in 0.2 ml of 50 μM KPi buffer (pH 7.4) containing 0.1 mM EDTA and 20% glycerol, then lysed by sonication. (**c**) 4-OH-IFA production by cultured cell lines. Cells were plated overnight in 12-well tissue culture plates at 150 000 cells per well and then incubated for 4 h in 1.5 ml fresh medium containing 0, 1 or 4 mM IFA plus 5 mM semicarbazide to stabilize the 4-hydroxy metabolite. An aliquot (0.5 ml) of culture medium was removed, derivatized and assayed for 4-OH-IFA formation and for relative cell number (crystal violet staining, A_{595}). Data shown are nmol 4-OH-IFA formed per A_{595} cell during the 4 h incubation (mean ± range, $n=2$). (**d**) Active MMDX metabolite formation, determined by the killing of 9L indicator cells in a 4-day growth inhibition assay. 9L indicator cells plated overnight at 3000 cells per well in 96-well plates were incubated for 4 days with cultured supernatants from 9L, 9L/3A4, CHO/HR, CHO/3A4 or CHO/3A4/HR cells incubated for 2 h with 2, 4 or 8 nM MMDX. 9L indicator cell killing expressed as a percentage of MMDX-free controls was determined by crystal violet staining (mean ± range, $n=2$). CHO/3A4-4 and CHO/3A4-10 correspond to two independent clones with similar CYP3A4 protein levels (not shown) and similar sensitivity to MMDX (see Table 1). IFA, ifosfamide; MMDX, methoxymorpholinyl doxorubicin.

route, although a modest but transient growth inhibitory effect was apparent in the case of the i.t. treatment group 3 days after the second MMDX injection (Figure 4a, inset). In contrast, 9L/3A4 tumors exhibited a substantial and prolonged regression following the first MMDX treatment cycle, either by the i.v. or by the i.t. route (Figure 4a and Table 2). Regrowth of the MMDX-treated 9L/3A4 tumors was not apparent until day 35, at which time a second cycle of three weekly MMDX treatments was initiated. Four of the eight tumors in this group did not double in size by the time the experiment was terminated on day 59; the doubling time for the other four tumors was 35 days for the first cycle of MMDX treatment and 17 days for the second MMDX treatment cycle, that is, six- and threefold longer than the 5.8-day doubling time of untreated 9L/3A4 tumors.

In separate experiments, mice bearing 9L/3A4 tumors were treated with MMDX by an i.p. injection every 6 days, either as a series of five injections at 40 μg per kg body weight or a series of four injections at 60 μg per kg body weight. No antitumor activity, and no host toxicity, was seen with the i.p. route of MMDX administration (Table 2). In contrast, i.v. MMDX treatment induced strong systemic toxicity, with four out of four mice dying within 7 days (9L tumors) and three out of four mice dying within 10 days (9L/3A4 tumors) after completing the first MMDX treatment cycle (Figure 4a and Table 2). This toxicity was also apparent from the body weight loss of 3–7 g seen for the 9L and 9L/3A4 tumor-bearing mice following i.v. MMDX injection (Figure 4b). Although a 2–4 g body weight loss was observed in the 9L/3A4 tumor-bearing mice on days 10 and 17 after the first i.t.

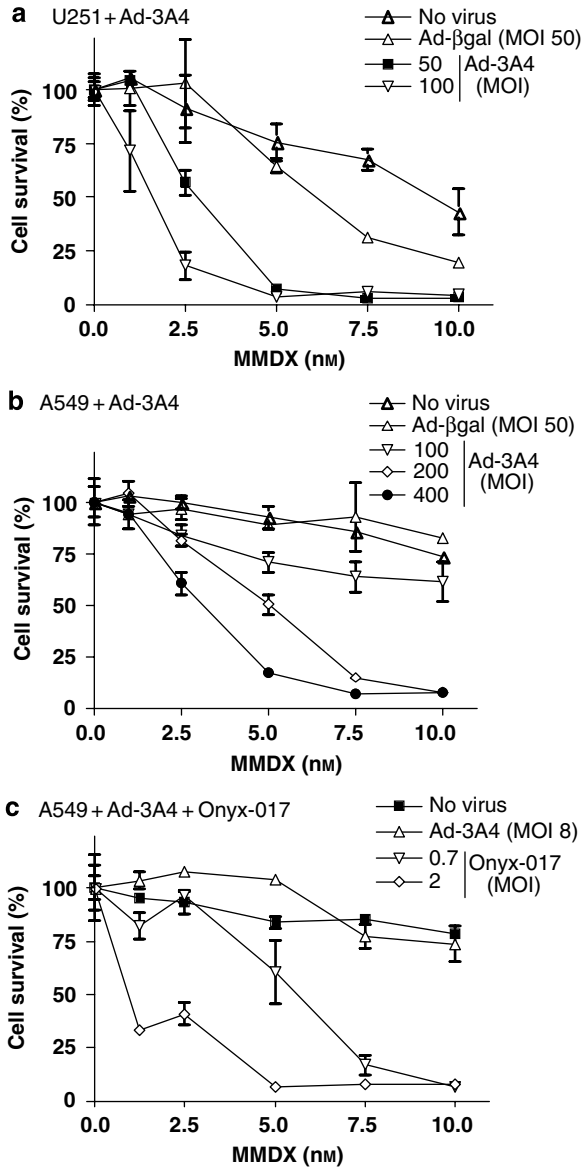

Figure 3 Cytotoxicity of MMDX toward Adeno-3A4-infected U251 (**a**) and A549 cells (**b** and **c**), without (**a** and **b**) or with (**c**) Onyx-017 coinfection. Cells seeded overnight in 24-well plates (14 000 cells per well) were infected with Adeno-3A4 or Adeno-βgal at the indicated MOI for 24 h, either alone (**a** and **b**) or in combination with Onyx-017 ((**c**); at MOIs 0.7 and 2). Cells were treated with MMDX in fresh culture medium at the indicated concentrations beginning 24 h after infection. The culture medium was replaced with medium containing fresh MMDX 2 days later to minimize the intrinsic toxicity of the virus, and the incubation was continued for an additional 5 days (total of 7 days MMDX treatment). Data are expressed as percent cell survival compared with the corresponding drug-free controls, determined by crystal violet staining, mean ± s.d. ($n=3$). In the absence of MMDX, Adeno-3A4 was moderately toxic to U251 cells ($\leqslant$30% cell killing at MOIs 50 and 100) but not to A549 cells ($<$16% killing at MOIs 200 and 400) (data not shown). The IC_{50} (MMDX) in A549 cells was 1 nM at 8 MOI Adeno-3A4 + 2 MOI Onyx-017 vs no effect in A459 cells infected with 8 MOI Adeno-3A4 alone. MMDX, methoxymorpholinyl doxorubicin; MOI, multiplicity of infection.

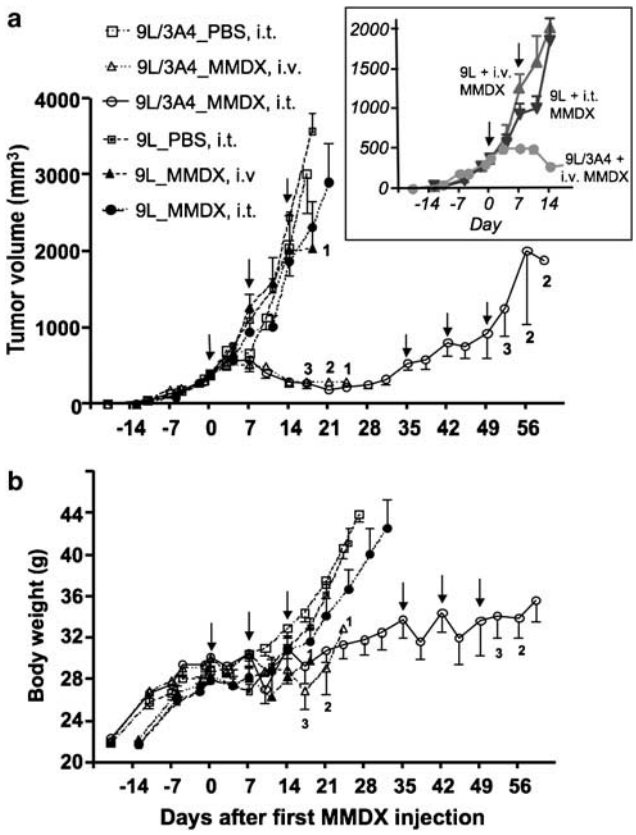

Figure 4 Tumor growth delay induced by MMDX in scid mice bearing 9L and 9L/3A4 tumors. 9L and 9L/3A4 tumors were implanted subcutaneously and grown in male scid mice. Tumor volume (**a**) and body weight (**b**) were measured twice a week. In the absence of drug treatment, 9L/3A4 tumors grew somewhat slower than 9L tumors (doubling time of 5.8 vs 4.6 days; Table 2), as was observed for the corresponding cell lines in culture (data not shown). Arrows indicate days on which each of three weekly doses of MMDX (60 μg kg^{-1}) was administered, either by i.v. or by i.t. injection, as indicated, beginning when the tumors reached 300–400 mm^3 in size. Numbers shown alongside individual data points indicate the number of mice remaining alive at each time point; data points not numbered indicate no deaths occurred, that is, four mice alive/drug-treated group. Tumor volume and body weight data are mean ± s.e. values based on $n=6$ tumors ($n=3$ mice) (drug-free controls) or $n=8$ tumors ($n=4$ mice) (MMDX treatment groups). MMDX was highly toxic by the i.v. administration route, with four out of four i.v. injected 9L tumor-bearing mice dying by day 21 (that is, 7 days after completing the cycle of three weekly MMDX injections) and three out of four i.v. MMDX-injected 9L/3A4 tumor-bearing mice dying by day 24. Drug toxicity was not observed for the i.t. MMDX 9L/3A4 tumor group until after completion of a second cycle of three weekly MMDX injections, with one mouse dying on day 52 and a second mouse on day 56. The inset in (**a**) highlights the transient growth delay seen in 9L tumors given MMDX by i.t. injection. I.t., intratumoral; i.v., intravenous; MMDX, methoxymorpholinyl doxorubicin.

MMDX injection, body weights recovered and no drug-induced deaths occurred (Figure 4b). Some toxicity was observed after the second cycle of i.t. MMDX treatment, with two mice dying after the third MMDX injection. Thus, MMDX given by direct i.t. delivery is effective in regressing 9L tumors that express CYP3A4, with drama-

Table 2 Effect of MMDX treatment on tumor-doubling time, tumor regression and host toxicity

Tumor	*MMDX dosing regimen*	*Dosing route*	*MMDX dose ($\mu g\,kg^{-1}$)*	*Doubling time (day)*	*Tumor regression (%)*	*Toxicity*
9L	q7d × 3	i.t.	0	4.6	0	0/3
9L	q6d × 5	i.p.	60	5.9	0	0/10
9L	q7d × 3	i.t.	60	6.5	0	0/4
9L	q7d × 3	i.v.	60	4.9	0	4/4
9L/3A4	q6d × 4	i.p.	0	4.7	0	0/2
9L/3A4	q7d × 3	i.t.	0	5.8	0	0/3
9L/3A4	q6d × 5	i.p.	40	5.7	0	0/10
9L/3A4	q6d × 4	i.p.	60	6.3	0	0/2
9L/3A4	q7d × 3	i.t.	60	~39	57	0/4
9L/3A4	q7d × 3	i.v.	60	~38	>46	3/4

Abbreviations: i.t., intratumoral; i.p., intraperitoneal; i.v., intravenous; MMDX, methoxymorpholinyl doxorubicin.
9L and 9L/3A4 tumors grown in scid mice, as in Figure 4, were treated with MMDX using the indicated dosing regimen, route and dose. Tumor-doubling time corresponds to the time in days required for the tumor volume to double relative to the volume on day 0, that is, the first day of MMDX treatment. Tumor regression was calculated as described in Materials and methods. Toxicity indicates the number of mice that died over the course of a cycle of MMDX treatment (that is, a series of three, four or five MMDX injections spaced 6 or 7 days apart, as indicated under dosing regimen) compared with the total number of treated animals, which ranged from 2 to 10, as shown in the last column.

tically decreased host toxicity compared with i.v. drug treatment.

Discussion

CYP3A4 is the major CYP in human liver, where it plays a dominant role in the metabolism of several anticancer drugs, including epipodophyllotoxins, tamoxifen, taxol, vinca alkaloids and IFA.[35] Drugs such as vinca alkaloids and irinotecan are metabolized by CYP3A4 to less active or inactive metabolites,[36,37] whereas other anticancer drugs, including IFA,[32] the bioreductive agent AQ4N[19] and the anthracycline MMDX, are metabolized by CYP3A4 to more toxic metabolites. These and other anticancer *P*450 prodrugs are potential candidates for use in *P*450-based gene therapy for cancer.[38] Preclinical *P*450 prodrug-activation studies to date have focused on CYP2B enzymes in combination with cyclophosphamide and IFA, and initial clinical trials have been promising.[15,39] However, the therapeutic potential of other *P*450–prodrug combinations, in particular those that involve CYP3A enzymes, which are distinguished from CYP2B enzymes by their high level expression in liver, is largely unknown. This study investigated whether CYP3A4 may be used together with the CYP3A prodrug MMDX for gene-directed enzyme prodrug therapy (GDEPT) applications in cancer. Our primary goal was to determine whether *CYP3A4* can be delivered to tumor cells at a level that is sufficient to sensitize the cells to MMDX, not only in cell culture, but also *in vivo*, where MMDX is extensively metabolized in the liver by endogenous hepatic CYP3A enzymes.

MMDX has several features that make it an attractive prodrug candidate for GDEPT applications. In particular, the cell membrane permeability[24] and long half-life of activated MMDX[27] both indicate that the activated metabolite has the potential to confer a strong bystander effect, which is essential for any GDEPT strategy to be effective *in vivo*. The potential utility of MMDX for GDEPT for cancer treatment was investigated using CYP3A4, which displays the highest rate of MMDX activation in a panel of CYP3A enzymes.[27] A 120-fold increase in MMDX sensitivity was obtained in 9L gliosarcoma cells infected with retrovirus expressing CYP3A4 as compared with CYP3A4-deficient 9L cell controls. Tumor cell expression of CYP3A4 dramatically increased chemosensitivity to MMDX *in vivo*, as revealed by a tumor growth delay study carried out in a scid mouse xenograft model. Notably, i.t. expression of CYP3A4 increased MMDX antitumor activity dramatically, even though MMDX itself has a substantial intrinsic anticancer activity, and despite the fact that MMDX-activating CYP3A enzymes are already expressed endogenously at a high level in mouse liver,[28] as they are in human liver.[27] CYP3A4, in combination with MMDX, is thus a promising enzyme–prodrug combination that warrants further development and preclinical evaluation. The strong chemosensitization of 9L/3A4 tumors to MMDX reported here further suggests that MMDX may be particularly active against tumors that express CYP3A4 endogenously, that is, without the introduction of a gene therapy vector. CYP3A4 expression has been reported in a broad range of primary human tumor tissues including those from patients with colon cancer,[40] breast cancer,[41] lung cancer,[42] renal cell cancer[43] and bladder cancer.[44] MMDX could be an agent of choice for patients with tumors characterized by high CYP3A4 levels, insofar as those tumors are likely to be resistant to drugs such as irinotecan/CPT-11, paclitaxel and docetaxel, which are inactivated by CYP3A4 metabolism.[36,40,45]

CYP3A4-expressing 9L cells grew approximately two-fold slower in culture than the corresponding *P*450-deficient cells. Slower growth rates were also reported in response to the introduction of CYP3A4 in human

Caco-2 intestinal cells and HepG2 hepatoma cells, both derived from tissues that normally express CYP3A4 endogenously.[46,47] In the case of Caco-2/3A4 cells, cell growth improved with the loss of CYP3A4 during cell passage.[46] Cells with a high CYP3A4 activity may thus be at a growth disadvantage and ultimately be replaced by more rapidly proliferating cells with a lower level of CYP3A4. This hypothesis may help explain the difficulty we encountered in coexpressing CYP3A4 and *P*450 reductase at high levels in 9L cells, insofar as cells with a lower CYP3A4 metabolic activity (that is, cells that do not overexpress *P*450 reductase and/or have a low level of CYP3A4) may have a growth advantage over cells in the population with higher levels of CYP3A4 activity. Conceivably, high levels of CYP3A4 activity could slow cell growth by metabolizing an essential endogenous cell growth regulator. However, an increase in growth rate was not seen when 9L/3A4 cells were cultured in the presence of the CYP3A-selective inhibitor troleandomycin (10–100 μM) (data not shown). Further studies are needed to fully understand the effects of CYP3A4 expression on tumor cell growth and viability and their impact on efforts to induce CYP3A4 expression in human tumors *in vivo* using viral or other gene therapy vectors.

CHO/3A4/HR cells are characterized by a 31-fold increase in *P*450 reductase activity compared with CHO/3A4 cells, which translated into a 28-fold higher CYP3A4 metabolic activity (IFA 4-hydroxylation) and an 11-fold (MMDX) or 23-fold (IFA) increase in prodrug cytotoxicity (Table 1). These findings support our earlier observation that coexpression of *P*450 reductase with CYP2B1 or CYP2B6 substantially improves GDEPT activity when combined with cyclophosphamide or IFA treatment.[4,7] In some tumor cell lines, however, there may be minimal or even no improvement in CYP metabolic activity upon coexpression of *P*450 reductase,[48] perhaps due to an already high molar ratio of endogenous *P*450 reductase to exogenous CYP, which is expected to saturate CYP metabolic activity.[49] Efforts to use retroviruses to increase the level of *P*450 reductase in 9L/3A4 cells were unsuccessful and resulted in a decrease in CYP3A4 protein levels without an increase in MMDX toxicity (data not shown). A decrease in CYP3A4 protein content was also seen when *P*450 reductase was introduced into CHO/3A4 cells, although in this case a large increase in overall CYP3A metabolic activity was obtained (Figure 2 and Ding *et al*.[29]). Thus, the impact of *P*450 reductase gene transfer on tumor cell capacity for *P*450 prodrug activation may be dependent on the endogenous tumor cell level of *P*450 reductase and its relation to the overall tumor cell *P*450 protein content following introduction of the gene therapy vector. Gene therapy vectors that give high levels of *P*450 expression (for example, adenoviral vectors)[34] may be particularly demanding in terms of the requirement for *P*450 reductase, particularly in the case of CYPs that have a low apparent affinity for *P*450 reductase.[50] The expression in tumor cells of other enzymes that utilize endogenous *P*450 reductase, which include cytochrome b_5, heme oxygenase and the fatty acid hydroxylation system, may also influence the requirement of exogenous *P*450 reductase for efficient GDEPT activity.

The toxicity of activated MMDX is manifest at nanomolar prodrug concentrations, which enabled us to carry out these studies at concentrations of MMDX that are >10 000-fold lower than the K_m for MMDX, 16 μM.[25] Nevertheless, despite the very low concentration of MMDX, there is sufficient formation of the active MMDX metabolite to affect tumor cell killing. This high potency of MMDX was retained *in vivo*, where low drug doses (60 μg per kg body weight) induced a substantial antitumor response, despite the fact that circulating MMDX concentrations are typically <10 nM following bolus MMDX administration,[51] that is, >1000-fold lower than the K_m (MMDX) for CYP3A4 metabolism. In contrast, IFA cytotoxicity required millimolar concentrations of prodrug, consistent with the K_m (IFA) of ~1 mM exhibited by CYP3A4.[32]

Human tumor cells infected with Adeno-3A4 exhibited a modest increase in MMDX sensitivity compared with that seen in the case of the retrovirus-infected 9L cells. Efforts to further chemosensitize the tumor cells using the tumor cell-replicating adenovirus Onyx-017 to promote the replication and increase the expression from the replication-defective adenoviral *P*450 vector[6,34] were only partially successful. Although coinfection of tumor cells with Onyx-017 + Adeno-3A4 resulted in a 50- to 60-fold increase in CYP3A4 RNA compared with Adeno-3A4 infection alone, only modest increases in CYP3A4 protein and activity were achieved. Further study will be needed to develop strategies for increasing i.t. CYP3A4 protein and activity *in vivo*, for example, by taking advantage of the recently described stabilizing effect of NFκB on CYP3A4 protein,[52] before this CYP3A4 gene therapy can be implemented in the clinic. Nevertheless, this study provides proof-of-concept for the potential of *CYP3A4* for prodrug activation-based gene therapy in the context of a high background of liver CYP3A activity.

*P*450-based GDEPT using cyclophosphamide-activating CYP2B enzymes improves i.t. 4-OH-cyclophosphamide pharmacokinetics and enhances antitumor activity *in vivo*, with the greatest improvements obtained when cyclophosphamide is administered by direct i.t. injection.[53,54] In this study, host toxicity associated with MMDX treatment was dramatically decreased when MMDX was directly delivered into tumors using a syringe pump. 9L/3A4 tumors did not respond to MMDX administered by an i.p. injection, suggesting that there is a significant first-pass hepatic effect that not only leads to MMDX activation but also inactivates MMDX and/or its active metabolite. Low host toxicity was observed when MMDX was administered by direct i.t. injection, in contrast to i.v. MMDX treatment, which resulted in seven out of eight deaths after the first cycle of MMDX treatment, perhaps due to intrinsic toxicities associated with exposure to the unmetabolized parent drug. Direct i.t. delivery of MMDX might also help overcome the low efficiency of drug uptake that characterizes many solid tumors, although in this study there was no difference in 9L/3A4 antitumor activity

between i.v. and i.t. MMDX administrations. Although i.t. chemotherapy is not suitable for all solid tumors and may impose certain practical limitations, it has been used in the clinic for treatment of a number of diseases, including head and neck cancer, lung cancer and breast cancer,[55–57] and could prove to be particularly effective in the case of CYP3A4-expressing tumors and MMDX.

In summary, the present proof-of-concept studies establish the therapeutic efficacy of MMDX treatment in combination with CYP3A4 gene transfer and demonstrate the strong anticancer potential of this novel gene–prodrug combination. However, the efficiency of CYP3A4 protein expression in tumor cells needs to be improved for this strategy to be implemented in the clinic. These studies also highlight the importance of the level of tumor cell expression, rather than the level of hepatic CYP3A4 expression for effective chemotherapeutic responses to MMDX in the absence of a gene therapeutic and suggest that patient tumor biopsies should be screened for CYP3A4 protein levels to identify individuals who are most likely to benefit from treatment with MMDX and perhaps other CYP3A4 prodrugs.

Abbreviations

CYP or *P*450, cytochrome *P*450; DMEM, Dulbecco's modified Eagle's medium; FBS, fetal bovine serum; GDEPT, gene-directed enzyme prodrug therapy; IFA, ifosfamide; MMDX, methoxymorpholinyl doxorubin, also known as nemorubicin; MOI, multiplicity of infection.

Acknowledgements

We thank Jie Ma for assistance with intravenous injections and Dr Thomas Friedberg (University of Dundee) for providing CYP3A4 cDNA and CHO cells expressing CYP3A4. This study was supported in part by NIH grant CA49248 (to DJW).

References

1 Michael M, Doherty MM. Tumoral drug metabolism: overview and its implications for cancer therapy. *J Clin Oncol* 2005; **23**: 205–229.
2 Moolten FL. Drug sensitivity ('suicide') genes for selective cancer chemotherapy. *Cancer Gene Ther* 1994; **1**: 279–287.
3 Roy P, Waxman DJ. Activation of oxazaphosphorines by cytochrome *P*450: application to gene-directed enzyme prodrug therapy for cancer. *Toxicol In Vitro* 2006; **20**: 176–186.
4 Chen L, Yu LJ, Waxman DJ. Potentiation of cytochrome *P*450/cyclophosphamide-based cancer gene therapy by coexpression of the *P*450reductase gene. *Cancer Res* 1997; **57**: 4830–4837.
5 Chase M, Chung RY, Chiocca EA. An oncolytic viral mutant that delivers the CYP2B1 transgene and augments cyclophosphamide chemotherapy. *Nat Biotechnol* 1998; **16**: 444–448.
6 Jounaidi Y, Chen CS, Veal GJ, Waxman DJ. Enhanced antitumor activity of *P*450prodrug-based gene therapy using the low Km cyclophosphamide 4-hydroxylase *P*4502B11. *Mol Cancer Ther* 2006; **5**: 541–555.
7 Jounaidi Y, Hecht JE, Waxman DJ. Retroviral transfer of human cytochrome *P*450genes for oxazaphosphorine-based cancer gene therapy. *Cancer Res* 1998; **58**: 4391–4401.
8 Tyminski E, Leroy S, Terada K, Finkelstein DM, Hyatt JL, Danks MK *et al*. Brain tumor oncolysis with replication-conditional herpes simplex virus type 1 expressing the prodrug-activating genes, CYP2B1 and secreted human intestinal carboxylesterase, in combination with cyclophosphamide and irinotecan. *Cancer Res* 2005; **65**: 6850–6857.
9 Niculescu-Duvaz I, Springer CJ. Introduction to the background, principles, and state of the art in suicide gene therapy. *Mol Biotechnol* 2005; **30**: 71–88.
10 Zhang Y, Parker WB, Sorscher EJ, Ealick SE. PNP anticancer gene therapy. *Curr Top Med Chem* 2005; **5**: 1259–1274.
11 Searle PF, Chen MJ, Hu L, Race PR, Lovering AL, Grove JI *et al*. Nitroreductase: a prodrug-activating enzyme for cancer gene therapy. *Clin Exp Pharmacol Physiol* 2004; **31**: 811–816.
12 Trask TW, Trask RP, Aguilar-Cordova E, Shine HD, Wyde PR, Goodman JC *et al*. Phase I study of adenoviral delivery of the HSV-tk gene and ganciclovir administration in patients with current malignant brain tumors. *Mol Ther* 2000; **1**: 195–203.
13 Cunningham C, Nemunaitis J. A phase I trial of genetically modified *Salmonella typhimurium* expressing cytosine deaminase (TAPET-CD, VNP20029) administered by intratumoral injection in combination with 5-fluorocytosine for patients with advanced or metastatic cancer. Protocol no: CL-017. Version: April 9, 2001. *Hum Gene Ther* 2001; **12**: 1594–1596.
14 Freytag SO, Stricker H, Peabody J, Pegg J, Paielli D, Movsas B *et al*. Five-year follow-up of trial of replication-competent adenovirus-mediated suicide gene therapy for treatment of prostate cancer. *Mol Ther* 2007; **15**: 636–642.
15 Braybrooke JP, Slade A, Deplanque G, Harrop R, Madhusudan S, Forster MD *et al*. Phase I study of MetXia-*P*450gene therapy and oral cyclophosphamide for patients with advanced breast cancer or melanoma. *Clin Cancer Res* 2005; **11**: 1512–1520.
16 Chen L, Waxman DJ. Intratumoral activation and enhanced chemotherapeutic effect of oxazaphosphorines following cytochrome P-450 gene transfer: development of a combined chemotherapy/cancer gene therapy strategy. *Cancer Res* 1995; **55**: 581–589.
17 Samel S, Keese M, Lux A, Jesnowski R, Prosst R, Saller R *et al*. Peritoneal cancer treatment with CYP2B1 transfected, microencapsulated cells and ifosfamide. *Cancer Gene Ther* 2006; **13**: 65–73.
18 Jounaidi Y, Waxman DJ. Combination of the bioreductive drug tirapazamine with the chemotherapeutic prodrug cyclophosphamide for *P*450/*P*450-reductase-based cancer gene therapy. *Cancer Res* 2000; **60**: 3761–3769.
19 McCarthy HO, Yakkundi A, McErlane V, Hughes CM, Keilty G, Murray M *et al*. Bioreductive GDEPT using cytochrome *P*4503A4 in combination with AQ4N. *Cancer Gene Ther* 2003; **10**: 40–48.
20 Ghielmini M, Colli E, Bosshard G, Pennella G, Geroni C, Torri V *et al*. Hematotoxicity on human bone marrow- and umbilical cord blood-derived progenitor cells and *in vitro* therapeutic index of methoxymorpholinyldoxorubicin and its metabolites. *Cancer Chemother Pharmacol* 1998; **42**: 235–240.
21 Kuhl JS, Duran GE, Chao NJ, Sikic BI. Effects of the methoxymorpholino derivative of doxorubicin and its

bioactivated form versus doxorubicin on human leukemia and lymphoma cell lines and normal bone marrow. *Cancer Chemother Pharmacol* 1993; **33**: 10–16.
22 Lau DH, Duran GE, Lewis AD, Sikic BI. Metabolic conversion of methoxymorpholinyl doxorubicin: from a DNA strand breaker to a DNA cross-linker. *Br J Cancer* 1994; **70**: 79–84.
23 Lewis AD, Lau DH, Duran GE, Wolf CR, Sikic BI. Role of cytochrome P-450 from the human CYP3A gene family in the potentiation of morpholino doxorubicin by human liver microsomes. *Cancer Res* 1992; **52**: 4379–4384.
24 Baldwin A, Huang Z, Jounaidi Y, Waxman DJ. Identification of novel enzyme–prodrug combinations for use in cytochrome *P*450-based gene therapy for cancer. *Arch Biochem Biophys* 2003; **409**: 197–206.
25 Quintieri L, Geroni C, Fantin M, Battaglia R, Rosato A, Speed W *et al*. Formation and antitumor activity of PNU-159682, a major metabolite of nemorubicin in human liver microsomes. *Clin Cancer Res* 2005; **11**: 1608–1617.
26 Alvino E, Gilberti S, Cantagallo D, Massoud R, Gatteschi A, Tentori L *et al*. *In vitro* antitumor activity of 3′-desamino-3′(2-methoxy-4-morpholinyl) doxorubicin on human melanoma cells sensitive or resistant to triazene compounds. *Cancer Chemother Pharmacol* 1997; **40**: 180–184.
27 Lu H, Waxman DJ. Antitumor activity of methoxymorpholinyl doxorubicin: potentiation by cytochrome *P*4503A metabolism. *Mol Pharmacol* 2005; **67**: 212–219.
28 Quintieri L, Rosato A, Napoli E, Sola F, Geroni C, Floreani M *et al*. *In vivo* antitumor activity and host toxicity of methoxymorpholinyl doxorubicin: role of cytochrome *P*4503A. *Cancer Res* 2000; **60**: 3232–3238.
29 Ding S, Yao D, Burchell B, Wolf CR, Friedberg T. High levels of recombinant CYP3A4 expression in Chinese hamster ovary cells are modulated by coexpressed human *P*450reductase and hemin supplementation. *Arch Biochem Biophys* 1997; **348**: 403–410.
30 Kozak M. Point mutations define a sequence flanking the AUG initiator codon that modulates translation by eukaryotic ribosomes. *Cell* 1986; **44**: 283–292.
31 Finer MH, Dull TJ, Qin L, Farson D, Roberts MR. kat: a high-efficiency retroviral transduction system for primary human T lymphocytes. *Blood* 1994; **83**: 43–50.
32 Chen CS, Jounaidi Y, Waxman DJ. Enantioselective metabolism and cytotoxicity of R-ifosfamide and S-ifosfamide by tumor cell-expressed cytochromes *P*450. *Drug Metab Dispos* 2005; **33**: 1261–1267.
33 Miwa GT, West SB, Lu AY. Studies on the rate-limiting enzyme component in the microsomal monooxygenase system. Incorporation of purified NADPH-cytochrome *c* reductase and cytochrome P-450 into rat liver microsomes. *J Biol Chem* 1978; **253**: 1921–1929.
34 Jounaidi Y, Waxman DJ. Use of replication-conditional adenovirus as a helper system to enhance delivery of *P*450prodrug-activation genes for cancer therapy. *Cancer Res* 2004; **64**: 292–303.
35 Kivisto KT, Kroemer HK, Eichelbaum M. The role of human cytochrome *P*450enzymes in the metabolism of anticancer agents: implications for drug interactions. *Br J Clin Pharmacol* 1995; **40**: 523–530.
36 Haaz MC, Rivory L, Riche C, Vernillet L, Robert J. Metabolism of irinotecan (CPT-11) by human hepatic microsomes: participation of cytochrome P-450 3A and drug interactions. *Cancer Res* 1998; **58**: 468–472.
37 Yao D, Ding S, Burchell B, Wolf CR, Friedberg T. Detoxication of vinca alkaloids by human *P*450CYP3A4-mediated metabolism: implications for the development of drug resistance. *J Pharmacol Exp Ther* 2000; **294**: 387–395.
38 Chen L, Waxman DJ. Cytochrome *P*450gene-directed enzyme prodrug therapy (GDEPT) for cancer. *Curr Pharm Des* 2002; **8**: 1405–1416.
39 Salmons B, Lohr M, Gunzburg WH. Treatment of inoperable pancreatic carcinoma using a cell-based local chemotherapy: results of a phase I/II clinical trial. *J Gastroenterol* 2003; **38**(Suppl 15): 78–84.
40 Martinez C, Garcia-Martin E, Pizarro RM, Garcia-Gamito FJ, Agundez JA. Expression of paclitaxel-inactivating CYP3A activity in human colorectal cancer: implications for drug therapy. *Br J Cancer* 2002; **87**: 681–686.
41 Schmidt R, Baumann F, Knupfer H, Brauckhoff M, Horn LC, Schönfelder M *et al*. CYP3A4, CYP2C9 and CYP2B6 expression and ifosfamide turnover in breast cancer tissue microsomes. *Br J Cancer* 2004; **90**: 911–916.
42 Kivisto KT, Fritz P, Linder A, Friedel G, Beaune P, Kroemer HK. Immunohistochemical localization of cytochrome *P*4503A in human pulmonary carcinomas and normal bronchial tissue. *Histochem Cell Biol* 1995; **103**: 25–29.
43 Murray GI, McFadyen MC, Mitchell RT, Cheung YL, Kerr AC, Melvin WT. Cytochrome *P*450CYP3A in human renal cell cancer. *Br J Cancer* 1999; **79**: 1836–1842.
44 Murray GI, Taylor VE, McKay JA, Weaver RJ, Ewen SW, Melvin WT *et al*. Expression of xenobiotic metabolizing enzymes in tumours of the urinary bladder. *Int J Exp Pathol* 1995; **76**: 271–276.
45 Engels FK, Ten Tije AJ, Baker SD, Lee CK, Loos WJ, Vulto AG *et al*. Effect of cytochrome *P*4503A4 inhibition on the pharmacokinetics of docetaxel. *Clin Pharmacol Ther* 2004; **75**: 448–454.
46 Crespi CL, Penman BW, Hu M. Development of Caco-2 cells expressing high levels of cDNA-derived cytochrome *P*4503A4. *Pharm Res* 1996; **13**: 1635–1641.
47 Yoshitomi S, Ikemoto K, Takahashi J, Miki H, Namba M, Asahi S. Establishment of the transformants expressing human cytochrome *P*450subtypes in HepG2, and their applications on drug metabolism and toxicology. *Toxicol In Vitro* 2001; **15**: 245–256.
48 Lengler J, Omann M, Duvier D, Holzmüller H, Gregor W, Salmons B *et al*. Cytochrome *P*450reductase dependent inhibition of cytochrome *P*4502B1 activity: implications for gene directed enzyme prodrug therapy. *Biochem Pharmacol* 2006; **72**: 893–901.
49 Kaminsky LS, Guengerich FP. Cytochrome P-450 isozyme/isozyme functional interactions and NADPH–cytochrome P-450 reductase concentrations as factors in microsomal metabolism of warfarin. *Eur J Biochem* 1985; **149**: 479–489.
50 Shimada T, Mernaugh RL, Guengerich FP. Interactions of mammalian cytochrome *P*450, NADPH-cytochrome *P*450reductase, and cytochrome b(5) enzymes. *Arch Biochem Biophys* 2005; **435**: 207–216.
51 Vasey PA, Bissett D, Strolin-Benedetti M, Poggesi I, Breda M, Adams L *et al*. Phase I clinical and pharmacokinetic study of 3′-deamino-3′-(2-methoxy-4-morpholinyl)doxorubicin (FCE 23762). *Cancer Res* 1995; **55**: 2090–2096.
52 Zangar RC, Bollinger N, Verma S, Karin NJ, Lu Y. The nuclear factor-kappa B pathway regulates cytochrome *P*4503A4 protein stability. *Mol Pharmacol* 2008; **73**: 1652–1658.
53 Chen CS, Jounaidi Y, Su T, Waxman DJ. Enhancement of intratumoral cyclophosphamide pharmacokinetics and antitumor activity in a *P*4502B11-based cancer gene therapy model. *Cancer Gene Ther* 2007; **14**: 935–944.

54 Ichikawa T, Petros WP, Ludeman SM, Fangmeier J, Hochberg FH, Colvin OM *et al*. Intraneoplastic polymer-based delivery of cyclophosphamide for intratumoral bioconversion by a replicating oncolytic viral vector. *Cancer Res* 2001; **61**: 864–868.
55 Duvillard C, Polycarpe E, Romanet P, Chauffert B. [Intratumoral chemotherapy: experimental data and applications to head and neck tumors]. *Ann Otolaryngol Chir Cervicofac* 2007; **124**: 53–60.
56 Celikoglu F, Celikoglu SI, Goldberg EP. Bronchoscopic intratumoral chemotherapy of lung cancer. *Lung Cancer* 2008; **61**: 1–12.
57 Almond BA, Hadba AR, Freeman ST, Cuevas BJ, York AM, Detrisac CJ *et al*. Efficacy of mitoxantrone-loaded albumin microspheres for intratumoral chemotherapy of breast cancer. *J Control Release* 2003; **91**: 147–155.

Supplementary Information accompanies the paper on Cancer Gene Therapy website (http://www.nature.com/cgt)